Introduction

After the discovery of electrospinning in 1934 [1], little research was conducted on electrostatically driven fluid jets for the next 35 years. In 1969 [2] a thorough experimental and theoretical study on the formation of electrostatically driven viscous jets consisting of both conducting and non-conducting monomeric fluids was undertaken. That study determined the minimum voltage necessary to expel the monomeric fluid from the tip of a needle as well as how the geometry of the pendant droplet varied with the electric field. In 1971, Baumgarten examined the factors influencing the electrospinning of acrylic polymers [3] and showed that the acceleration of the fluid jet during electrospinning varies proportionally with the dielectric constant of the solution being electrospun. It thus became known that polymer solutions with higher dielectric constants are more conducive to electrospinning compared to those with lower dielectric constants.

Over two decades later the field was revitalized by Doshi and Reneker [4] when they reported the formation of fibers from an aqueous solution of poly(ethylene oxide) dissolved in water. The primary findings included the observation that the more concentrated the polymer solution was, the higher the necessary accelerating voltage needed to be. This was necessary for the electrostatic interactions to overcome the surface tension of the pendant droplet expelling the charged polymer solution jet. It was also discovered that the closer to the tip the electrospun poly(ethylene oxide) fibers were collected, the larger the resultant fiber diameters. Although this was only a basic study, it suggested that processing variables such as the tip-to-collector distance and applied potential as well as solution properties affect the formation and properties of electrospun fibers.

In an attempt to further elucidate the relationship between the solution variables and the morphology of the electrospun fibers, another study was conducted to determine why morphological defects such as beads and beaded fibers, shown in Figure 1, form during the electrospinning process [5]. It was discerned that the major factors affecting the formation of beads and beaded fibers in electrospun matrices include the viscosity of the solution being electrospun and the surface tension of the polymer solution. In this study, as the viscosity of the solution being electrospun increased, the transformation from beaded fibers to uniform fibers occurred; in addition, the higher the surface tension of the solution being electrospun the more likely the polymer solution jet would break up into polymer droplets (beads). The latter point can be understood by thinking about the polymer solution jet as a continuum. As the surface tension of the jet increases, so does the tendency for that jet to contract and act against the elongational effects of the electric field, making it susceptible to separation into beads.
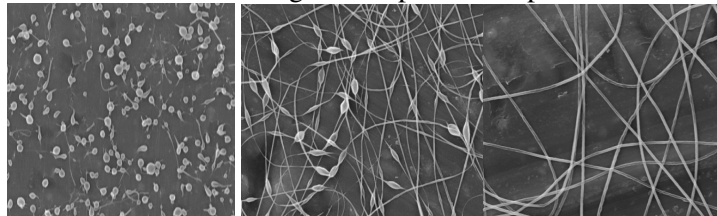

Figure 1. Field emission scanning electron microscopy (FE-SEM) images (left to right) of beads, beaded fibers and uniform fibers free of defects, reproduced from [5].

Motivation

Electrospinning is now recognized as an efficient technique to produce polymer fibers, with diameters ranging from tens of nanometers to tens of microns. Polymer micro- and nanofibers are fabricated from polymer solutions or melts using an electric field, which "shapes" the polymer into a fiber. The applications of electrospun polymer fibers have been wide spread, encompassing many pre-commercial applications including composites, filtration systems, medical prosthesis, tissue templates, electromagnetic shielding and liquid crystal devices [6].

A typical electrospinning setup usually consists of three components (Fig. 2), a syringe with or

without a needle, a collector and a high voltage supply. A polymer solution or low viscosity melt is fed to the tip of the needle by a syringe pump to form a droplet. The droplet is electrically charged by using the high voltage power supply to create a potential difference between the syringe/needle and the collector. The hemispherical shape of that droplet is then deformed into a conical geometry called a Taylor cone [2] by charges accumulated on the surface of the deformed droplet. Once the repulsive forces overcome the surface tension of the droplet, a
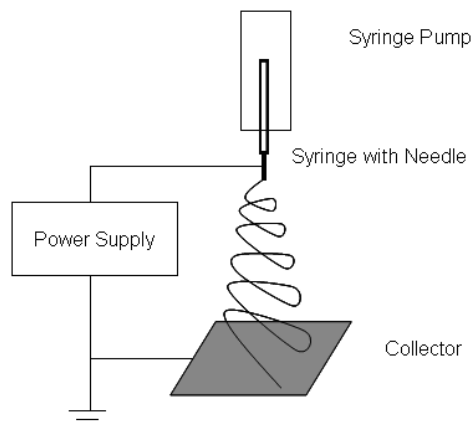

Figure 2. Schematic of a typical electrospinning apparatus

jet of polymer is emitted [4] and travels towards the collector. The charges on the electrified jet interact with each other and the electric field produced between the syringe and the collector, resulting in elongation and whipping of the jet. Meanwhile, due to the increasing surface to volume ratio (compared to a film), the solvent in the solution evaporates and solid polymer fibers are obtained on the collector. Production of a wide variety of polymeric nanofibers using electrospinning is now routine in many labs. The next step in this fiber production method involves controlling the molecular structure and chain orientation within the fiber, allowing for improved mechanical performance at the fiber level and consequently within the fibrous mat. We will focus on extending our initial work on controlling structure and orientation through the variation of spinning conditions coupled with the characterization tools we have developed for measurement of chain orientation and molecular structure and conformation under both static and dynamic conditions.

Chain orientation in electrospun fibers

Polyethyelene oxide (PEO) nanofibers were successfully aligned [7] by electrospinning between two electrically charged aluminum plates. The data obtained from the macroscopically unoriented and oriented electrospun nanofibers were compared using FE-SEM, polarized FTIR spectroscopy, polarized Raman spectroscopy and X-ray diffraction. Microscopic chain orientation along the fiber axis was observed. This represented the first observation of chain orientation in electrospun fibers using vibrational spectroscopy and suggested that both infrared and Raman measurements provide an easily applied characterization tool for the measurement of chain orientation once the electrospun fibers have been macroscopically aligned.

Real time measurement of chain orientation in electrospinning

Recently we have completed a feasibility study to detect the alignment of atactic PS (a-PS) chains during the electrospinning process using polarized Raman spectroscopy. During electrospinning, the region of the straight liquid jet emanating from the Taylor cone and the region near the onset of instability is of interest for characterizing elongational flow, since eventually the region downstream inhibits further

extension of polymer chains due to solidification (solvent evaporation). Several experimental and theoretical studies [8-10] over the years, propose a very high stretching region leading to uniaxial extension of the polymer jet.

The assignment of different vibrational modes of a-PS was first published by Liang et al. [11] and later refined by Jasse and Koenig [12]. The band at 1004 cm^{-1} was assigned to a phenyl ring vibration.and is very intense. The chain axis of an extended polystyrene molecule is along the methylene group (-CH-CH$_2$-CH-), while the C$_1$-C$_4$ phenyl ring axis is reported to be perpendicular to the chain axis. The normal to the phenyl ring lies at a 35° angle with respect to the chain axis. The radial skeletal ring vibration (623 cm^{-1}) of the aromatic group has been utilized to estimate the orientation parameters (P$_2$ & P$_4$) for uniaxially stretched a-PS.

Figure 3a and 3b contains the ZZ (black) and YY (red) polarized Raman spectra of isotropic and stretched PS samples, respectively. The bands of interest at 623 cm^{-1} and 1004 cm^{-1} are highlighted. In Figure 3c and 3d is shown the region of interest after normalization of the spectra with the 1004 cm^{-1} band. For an isotropic solvent cast film sample, no significant intensity differences of the bands are observed in the ZZ and YY polarization geometries, indicating that random orientation of the PS chains occurs as would be expected. However upon stretching the PS film, the intensity of the radial skeletal ring band at 623 cm^{-1} is larger in the YY spectrum than in the ZZ spectrum, indicating that alignment of aromatic ring planes perpendicular to the stretching direction has occurred. This is consistent with the studies by Jasse and Koenig [12] who observed that the aromatic ring plane aligns perpendicular to the stretching direction as the sample is drawn. Thus, in order to monitor the effect of electric field on the drawing of polymer chains during electrospinning of PS, the radial skeletal ring band (623 cm^{-1}) is utilized to understand the change in orientation of the PS chains in the straight jet region.
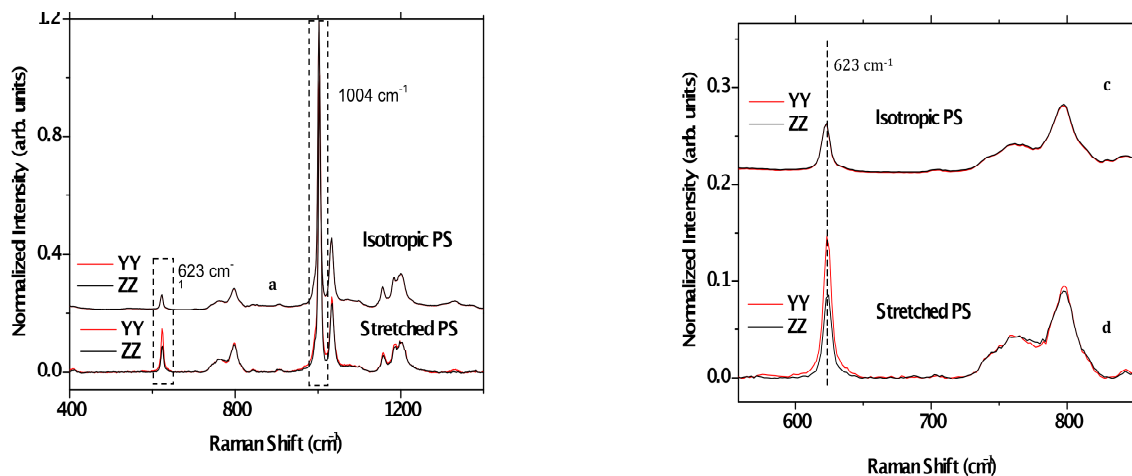

Figure 3. Polarized Raman spectra of PS films before and after stretching.

Figure 4 contains the first real-time, polarized Raman spectra obtained during electrospinning of a-PS nanofiber at the tip of the Taylor cone and at various distances along the unperturbed jet. The spectra were normalized to the 1004 cm^{-1} band for comparison. The normalized intensity of 623 cm^{-1} band in the YY polarization is not significantly different from the intensity in ZZ polarization at the location close to the tip. However, moving further down from the tip, at 5 mm distance, we note that the intensity of the 623 cm^{-1} band in the YY polarization is slightly higher than the intensity in the ZZ polarization. This intensity difference increases further and is significant at 9 mm and 14 mm below the tip. The difference in the intensities for ZZ and YY polarizations clearly indicate that anisotropy of the a-PS chains is induced in the electrospinning process. The aromatic ring of a-PS is aligned with the electric field in the jet region during the process. Thus, in addition to macroscopic changes such as thinning of the jet and a

decrease in fiber diameter, there is also significant molecular orientation due to high elongation caused by the electric field induced whipping action. This is consistent with the results observed in previous studies [9,10,13]. These report a sharp increase in axial stress in the initial phase of electrospinning (immediately near the tip), where the liquid jet undergoes thinning. Thus the polarized Raman experiments successfully measured the onset of chain orientation in the jet.
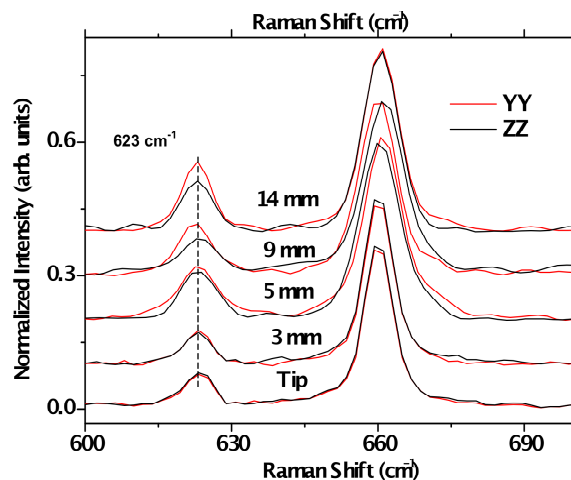

Figure 4. Real-time Polarized Raman spectra of PS during electrospinning. The numbers indicate the distance below the Taylor cone from which the spectra were recorded

Impact of solvent vapor on crystalline polymorphs in electrospun Nylon 6

The role of solvent evaporation on the crystalline state of conventionally electrospun Nylon 6 fibers was examined by electrospinning into a closed chamber filled with different concentrations of solvent vapor. Electrospun Nylon 6 fibers normally exhibit the metastable γ crystalline form. It was found that the thermodynamically stable α form became increasingly present in Nylon 6 fibers electrospun out of both 1,1,1,3,3,3-hexafluoro-2-propanol (HFIP) and formic acid as the vapor phase solvent concentration increased. It is believed that the formation of the metastable γ form is due to the fast solvent evaporation kinetics associated with the electrospinning process. By varying the vapor phase concentration and thus the rate of solvent evaporation during electrospinning, it was possible to control the resulting crystal structure of the electrospun Nylon 6, as shown by WAXD, Raman and FTIR spectroscopy [14].

Electrospinning nanofibers using an AFM tip

Nylon 6 nanofibers were successfully fabricated using an atomic force microscope probe (AFM) as an electrospinning tip. The nanometer-size tip enabled the controlled deposition of uniform polymeric nanofibers within a 1 cm diameter area. Nylon 6 nanofibers were continuously electrospun at a solution concentration as low as 1 wt % Nylon 6 in 1, 1, 1, 3, 3, 3-hexafluoro-2-propanol (HFIP). In addition, electrospun fibers from syringe-needle based electrospinning and AFM probe-tip based electrospinning were compared. Results indicated that significant morphological and microstructural differences had occurred in the case of AFM based electrospinning, possibly due to the role of surface charges and electric field strength. Electrospun fibers from both techniques display predominantly the metastable γ crystalline form; however wide-angle X-ray diffraction (WAXD) and differential scanning calorimetry (DSC) results show a small but significant decrease in melting point of the AFM spun fibers

demonstrating an effect either due to confinement in a cylindrical shape [16, 17] or the effect of process dynamics on crystal perfection due to solvent evaporation.

Conclusions

The ultimate mechanical properties of electrospun fibers and mats are a function of molecular level structure and chain orientation. Past work [18] has demonstrated that secondary structure and crystal structure can be affected by electrospinning conditions. Significantly less information has been available on chain orientation. Preliminary work [7] has already shown that chain orientation can be induced by changing the electrospinning conditions involving electric fields at the collector. Our studies have focussed on understanding the relationships between electrospinning conditions and chain orientation, as well as possible effects of cylindrical confinement in small diameter fibers on both secondary structure, crystal form and chain orientation . Our research is divided into both static and dynamic electrospinning characterization studies in an attempt to identify and assess the effect of various processing and collection strategies on molecular alignment and crystallization in polymer nanofibers.

References

[1] A. Formhals, 1934; US Patent 1,975,504 (1934).
[2] G.I. Taylor, Proc. Roy. Soc. London, A313 (1969) 453.
[3] P.K. Baumgarten, J. Coll. Inter. Sci. 36 (1971) 71.
[4] J. Doshi, D.H. Reneker, J. Electrostatics 35 (1995) 151.
[5] H. Fong, I. Chun, D.H. Reneker, Polymer 40 (1999) 4585.
[6] Z.M. Huang, Y.Z. Zhang, M. Kotaki, S. Ramakrishina; Composites Science and Technology ; 2003, 63 ,2223
[7] M.V. Kakade, S. Givens, K. Gardner, K.H. Lee, D.B. Bruce, J.F. Rabolt; Electric field induced orientation of polymer chains in macroscopically aligned electrospun polymer nanofibers, Journal of the American Chemistry Society; 2007, 129, 2777
[8] Helgeson, M. E.; Grammatikos, K. N.; Deitzel, J. M.; Wagner, N. J., Theory and kinematic measurements of the mechanics of stable electrospun polymer jets. *Polymer* **2008,** *49* (12), 2924-2936.
[9] Feng, J. J., Stretching of a straight electrically charged viscoelastic jet. *Journal of Non-Newtonian Fluid Mechanics* **2003,** *116* (1), 55-70.
[10] Colman P. Carroll, Y. L. J., Axisymmetric instabilities of electrically driven viscoelastic jets. *J. Non-Newtonian Fluid Mech.* **2008,** *153*.
[11] Liang, C. Y.; Krimm, S., Infrared spectra of high polymers. VI. Polystyrene. *Journal of Polymer Science* **1958,** *27* (115), 241-254.
[12]. Jasse, B.; Koenig, J. L., Polarized Raman study of molecular orientation in uniaxially stretched atactic polystyrene. *Journal of Polymer Science: Polymer Physics Edition* **1980,** *18* (4), 731-738.
[13] D. H. Reneker, A. Y., H. Fong and S. Koombhongse, *J. Appl. Phys.* **2000,** *87*.
[14] Carl B. Giller, Bruce Chase, John F. Rabolt and Christopher M. Snively, Effect of Solvent Evaporation Rate on the Crystalline State of Electrospun Nylon 6, *Polymer* **2010**, 51, 4225-4230
[15] G.Gururajan, S.P. Sullivan, T. P. Beebe, D.B.Chase and J.F.Rabolt, Continuous Electrospinning of Nylon 6 Nanofibers Using an Atomic Force Microscopy Probe Tip, *Soft Matter* (submitted 10/10)
[16] M. Steinhart, S. Senz, R. B. Wehrspohn, U. Gosele and J. H. Wendorff, Curvature Directed Crystallization of Poly(vinylidene difluoride) in Nanotube Walls, *Macromolecules* **2003**, *36*, 3646-3651.
[17] J. Lutkenhaus, K. McEnnis, A. Serghei and T. P. Russell. Confinement Effects on Crystallization and Curie Transitions of Poly9vinylidene fluoride-co-trifluoroethylene), *Macromolecules* **2010**, *43*, 3844-3850.
[18] Keun-Hyung Lee, Christopher M Snively, Steven Givens, D. Bruce Chase and John F. Rabolt, Time-dependent Transformation of an Electrospun Isotactic Poly(1-butene) Fibrous Membrane, *Macromolecules* **2007**, 40, 2590-259